

Microarticle

An integrated microring circuit design for optoelectronic transformer applications

J. Ali^a, P. Youplao^b, N. Pornsuwancharoen^b, K. Chaiwong^c, S. Chiangga^d, I.S. Amiri^e,
S. Punthawanunt^f, G. Singh^g, P. Yupapin^{h,i,*}, K.T.V. Grattan^j

^a Laser Centre, IBNU SINA ISIR, Universiti Teknologi Malaysia, 81310 Johor Bahru, Malaysia

^b Department of Electrical Engineering, Faculty of Industry and Technology, Rajamangala University of Technology Isan, Sakon Nakhon Campus, 199 Phungkon, Sakon Nakhon 47160, Thailand

^c Department of Electrical and Electronics Engineering, Faculty of Industrial Technology, Loei Rajabhat University, Loei 42000, Thailand

^d Department of Physics, Faculty of Science, Kasetsart University, Bangkok 10900, Thailand

^e Division of Materials Science and Engineering, Boston University, Boston, MA 02215, USA

^f Multidisciplinary Research Center, Faculty of Science and Technology, Kasem Bundit University, Bangkok 10250, Thailand

^g Department of Electronics and Communication Engineering, Malaviya National Institute of Technology Jaipur, 302017, India

^h Computational Optics Research Group, Advanced Institute of Materials Science, Ton Duc Thang University, District 7, Ho Chi Minh City, Viet Nam

ⁱ Faculty of Applied Sciences, Ton Duc Thang University, District 7, Ho Chi Minh City, 700000, Viet Nam

^j Department of Electrical & Electronic Engineering, School of Mathematics, Computer Science & Engineering, City, University of London, EC1V 0HB, United Kingdom

A B S T R A C T

The on-chip scale circuit of the optoelectronic transformer is designed and manipulated using the microring resonator system. By using the monochromatic input light source, the electro-optic signals can be generated and functioned as the step up and down conversion by mean of the on-chip optoelectronic transformer. The step up and down of the electro-optic related power conversions can be obtained via the input and drop port connections. The results obtained have shown that the flexible up and down electro-optic conversion ratios of 1: 5 and 10:1 for the step up and down conversions, respectively. The uses light source wavelength source was centered at 800 nm, where the conversion stability of 1600 fs is noted. The linearity trend of the conversion stability is confirmed.

Optoelectronic and plasmonic materials have become the most exciting goals for the new disrupted changes in modern advanced technologies. The advantages of such materials are the small dimension and the electro-optic signal conversion that can offer the various forms of applications [1–4], where the critical aspect is that the electrical and optical signal conversion can offer the challenging applications [5–8]. Recently, the authors in the references [9–14] have reported the promising works that the on-chip circuit of the electro-optic signal conversion can be integrated by a tiny circuit, which can offer the challenged application, especially, the electro-optic signal conversion. In this article, the optoelectronic transformer on-chip circuit is designed and manipulated. By using the optoelectronic material property, a circuit can be employed as the embedded part in the circuits, which is allowed the required up and down electrical voltages being arranged. By using the specific arrangement of the nonlinear microring circuits, the optoelectronic transformer can be obtained. The preliminary results can be obtained by using the Opti-wave program to manipulate and investigate the required signal characteristics, in which the selected device parameters of the results can be obtained and applied for the further improvements. The Matlab program is also employed for the

specific conditions of the required results.

From the system in Fig. 1, the input electrical field is given by $E_{in} = E_Z = E_0 e^{-ik_z Z - \omega t + \varphi}$ [15], Where E_0 is the initial electric field amplitude, k_z is the wave number in the direction of propagation, ω is

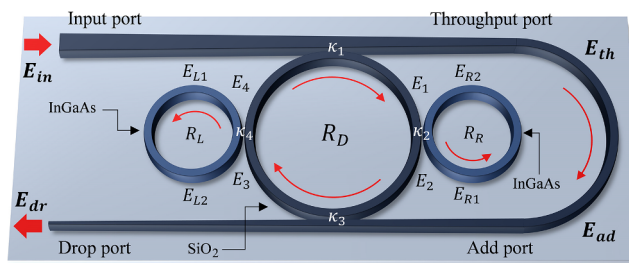


Fig. 1. An on-chip Optoelectronic Transformer circuit, where E_{in} , E_{th} , E_{dr} , E_{ad} are the electrical fields of the input, through, drop and add ports, R_R , R_L , and R_D are the right, the left, and the centre rings, respectively, all coupling coefficients are $\kappa_s = 0.5$. The center ring is a silicon oxide material, while the ring materials are the InGaAs and SiO_2 materials.

* Corresponding author.

E-mail address: preecha.yupapin@tdtu.edu.vn (P. Yupapin).

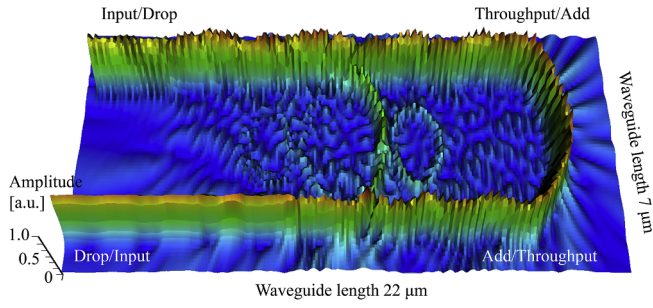


Fig. 2. The graphical results of the system, where the input light pulse power is 100 mW with the center wavelengths of 800 nm. The ring system, $R_L = R_R = 1.0 \mu\text{m}$, $R_D = 1.75 \mu\text{m}$. All κ_1 to $\kappa_4 = 0.5$. The InGaAs refractive index (n_0) is 2.9, the nonlinear refractive index (n_2) is $1.02 \times 10^{-17} \text{ m}^2 \text{ W}^{-1}$ [6–10], while n_{SiO_2} is 1.439. The used waveguide loss is 0.10 dB cm^{-1} , the core effective area is varied from 0.25 to $1.0 \mu\text{m}^2$.

the angular frequency, where φ is the initial phase. The distributed electrical fields within the system are given by

$$E_1 = \sqrt{1 - \gamma_1} \left(\sqrt{1 - \kappa_1} E_4 e^{-\frac{\alpha L_D}{2} - jk_n \frac{L_D}{2}} - j\sqrt{\kappa_1} E_{in} \right) \quad (1)$$

$$E_2 = \sqrt{1 - \gamma_2} \left(\sqrt{1 - \kappa_2} E_1 e^{-\frac{\alpha L_D}{2} - jk_n \frac{L_D}{4}} - j\sqrt{\kappa_2} E_{R2} e^{-\frac{\alpha L_R}{2} - jk_n \frac{L_R}{2}} \right) \quad (2)$$

$$E_3 = \sqrt{1 - \gamma_3} \left(\sqrt{1 - \kappa_3} E_2 e^{-\frac{\alpha L_D}{2} - jk_n \frac{L_D}{4}} - j\sqrt{\kappa_3} E_{th} \right) \quad (3)$$

$$E_4 = \sqrt{1 - \gamma_4} \left(\sqrt{1 - \kappa_4} E_3 e^{-\frac{\alpha L_D}{2} - jk_n \frac{L_D}{4}} - j\sqrt{\kappa_4} E_{L2} e^{-\frac{\alpha L_L}{2} - jk_n \frac{L_L}{2}} \right) \quad (4)$$

$$E_{th} = \sqrt{1 - \gamma_1} \left(\sqrt{1 - \kappa_1} E_{in} - j\sqrt{\kappa_1} E_4 e^{-\frac{\alpha L_D}{2} - jk_n \frac{L_D}{4}} \right) \quad (5)$$

$$E_{dr} = \sqrt{1 - \gamma_3} \left(\sqrt{1 - \kappa_3} E_{ad} - j\sqrt{\kappa_3} E_2 e^{-\frac{\alpha L_D}{2} - jk_n \frac{L_D}{4}} \right) \quad (6)$$

where $E_{ad} = E_{th}$. The circumference of the ring is L . L_R , L_L and L_D are the circumference of the right, left and center rings.

In a simulation, the selected light source with a wavelength of 800 nm is input into the input port as shown in Fig. 1. The related figure captions provide the other used parameters. In applications, the required input/output signal output can be configured by the device components, which can be supplied by the optoelectronic transformer in either the step-up or down requirements. The overall integrated circuit can be more complicated and reliable for various forms of applications. The graphical results of the optoelectronic transformer in

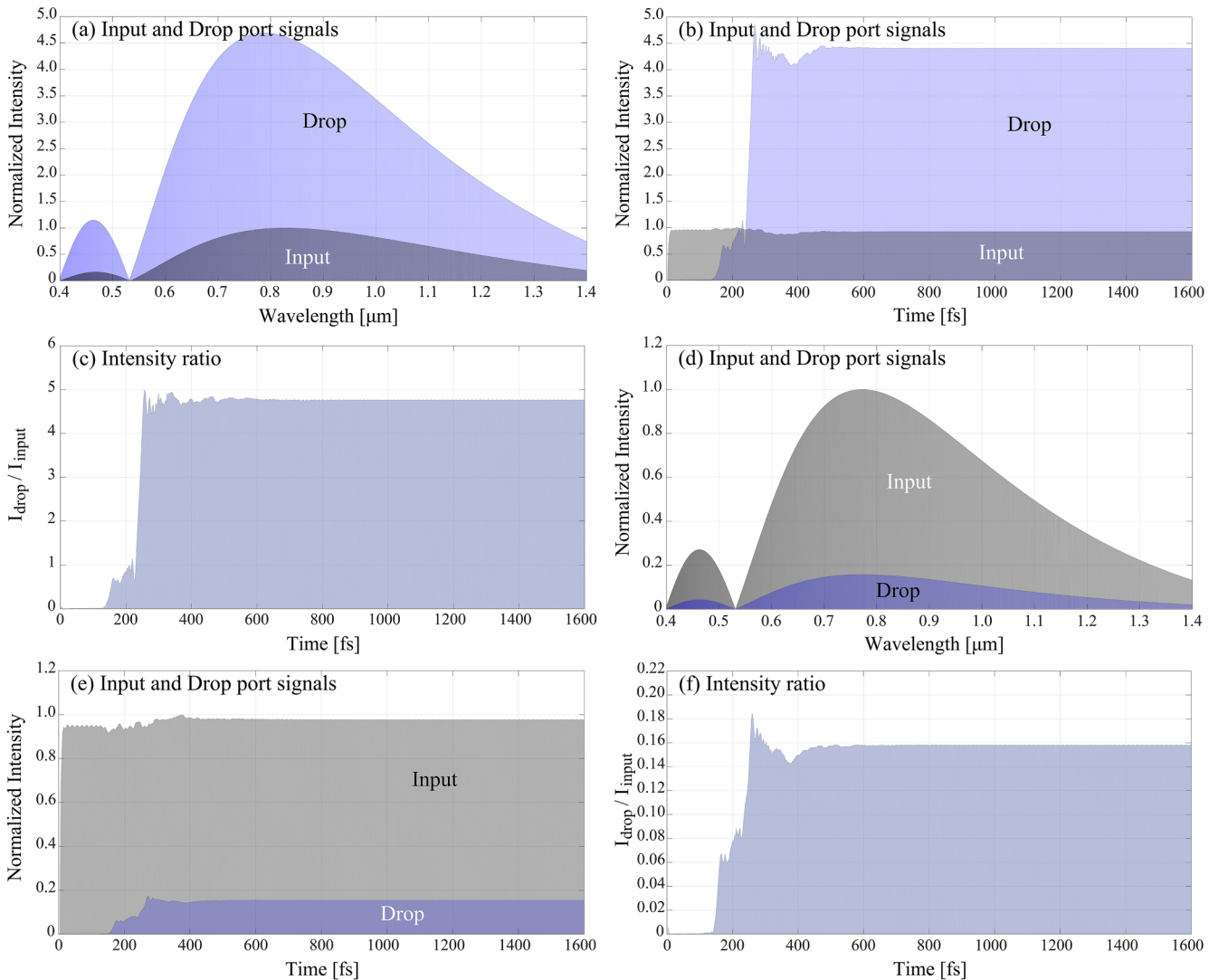


Fig. 3. Simulation results of the electro-optic conversion, where (a)–(c) and (d)–(f) are step-up and down conversions, where the input light power was fixed at 100 mW.

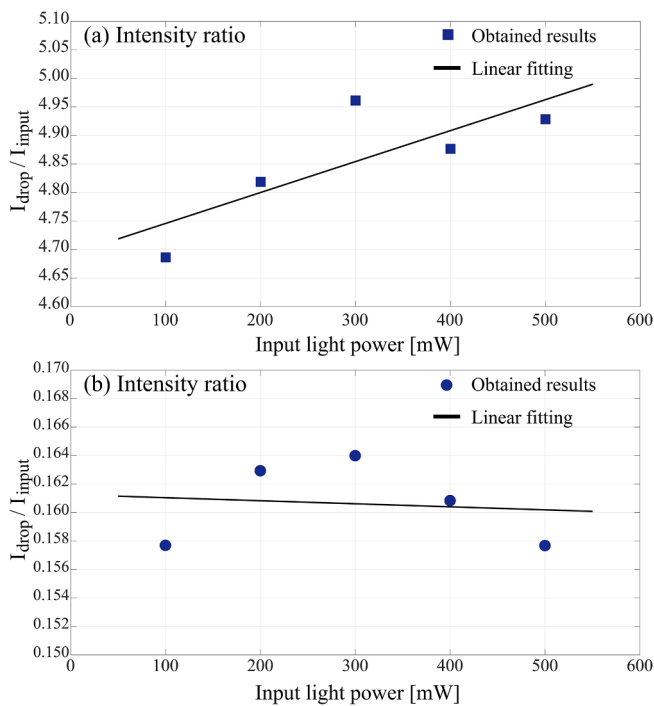


Fig. 4. The plots of the conversion stabilities of the results in Fig. 3, where (a) the step-up and (b) the step-down conversions.

Fig. 1 are as shown in Fig. 2, where the input light pulse power is 100 mW with the center wavelengths is at 800 nm. The ring radii are $R_L = R_R = 1.0 \mu\text{m}$, $R_D = 1.75 \mu\text{m}$. The applied program is the Optiwave. The center ring signals are coupled by the nonlinear side ring signals, in which the short coherence pulse of the side ring signals can be resonant with the center ring signals and the obtained peak signal power is higher within the shorter time, which means that the power per area is increased but the conservation of energy is maintained, which is detected at the throughput port. The extended results are obtained by the Matlab program as shown in Fig. 3, where the simulation results of the electro-optic conversion by using the selected parameters and given by the related figure captions, where (a)-(c) and (d)-(f) are the step-up and down conversions, respectively. The input light power was fixed at 100 mW. The comparison between the input and drop port normalized intensities and wavelength and time are plotted. The obtained results have shown that the promising results of the step-up and down conversion can be transformed with stability in time and wavelength. The ratios of the transformer of 1: 5 and 10:1 for the step up and down are noted. The stability time of 1600 fs is noted. The plots of the conversion stabilities of the results are shown in Fig. 3, where (a) the step-up and (b) the step-down conversions. The maximum input power of 600 mW was applied, where the linearity trends are seen (See Fig. 4).

We have proposed the use of the integrated microring circuit for an optoelectronic transformer, which is a micro-scale device that can be fabricated and on-chip application [16]. The selected light source was wavelength 800 nm, the microring materials were the InGaAs and SiO_2 materials. The center ring was formed by a SiO_2 , the side rings formed

by the InGaAs, in which the nonlinear effect was obtained by the high Kerr effect of the InGaAs, which is useful for short pulse pumping output requirement. The maximum pumping output for the step-up and down of 5 times is achieved. In application, the required power conversion of the input/output components within the applied plasmonic circuits can be employed with this form of the device, in which the specific input/output powers are required in the circuit operation.

Acknowledgments

The authors would like to give the appreciation for the research financial support and the research facilities and financial support from the Universiti Teknologi Malaysia, Johor Bahru, Malaysia through Flagship UTM shine project (03G82), Tier 1 (16H44) and Tier 2 (15J57) grants.

Appendix A. Supplementary data

Supplementary data to this article can be found online at <https://doi.org/10.1016/j.rinp.2018.10.022>.

References

- [1] Ginzburg P, Orenstein M. Plasmonic transmission lines: from micro to nano scale with $\lambda/4$ impedance matching. *Opt Express* 2007;15(11):6762–7.
- [2] Feng N-N, Negro LD. Plasmonic mode transformer using modulated-index metal-dielectric slot waveguides. *LEOS 2007-IEEE Laser and Electro-Optics Society, Annual Meeting Conference Proceedings* 2007:200–1.
- [3] Ozbay E. Plasmonics: merging photonics and electronics at the nanoscale dimensions. *Science* 2006;311(5738):189–93.
- [4] Raknoi P, Chiangga S, Amiri IS, Yupapin P. Array waveguide grating model for nanoparticle sensor applications. *Microsyst Technol* 2018:1–7.
- [5] Soysouvanh S, Jalil MA, Amiri IS, et al. Ultra-fast electro-optic switching control using a soliton pulse within a modified add-drop multiplexer. *Microsyst Technol* 2018;24(9):3777–82.
- [6] Atabaki AH, Moazenni S, Pavanello F, et al. Integrating photonics with silicon nanoelectronics for next generation of system on a chip. *Nature* 2018;556:349–54.
- [7] Koos C, Jacome L, Poulton C, et al. Nonlinear silicon-on-insulator waveguides for all-optical signal processing. *Opt Express* 2007;15:5976–90.
- [8] Hourhout DV, Baets R. Silicon micro-ring resonators. *Laser Photon. Rev.* 2012;6(9):47–73.
- [9] Ali J, Youplao P, Pornsuwancharoen N, et al. On-chip remote charger model using plasmonic island circuit. *Results Phys* 2018;9:815–8.
- [10] Pornsuwancharoen N, Youplao P, Aziz MS, et al. In-situ 3D micro-sensor model using embedded plasmonic island for biosensors. *Microsyst Technol* 2018;24(9):3631–5.
- [11] Pornsuwancharoen N, Youplao P, Chaiwong K, et al. Manual control of optical tweezer switching for particle trapping and injection. *IET Micro Nano Lett* 2018;13(7):911–4.
- [12] Punthawanunt S, Aziz MS, Phatharacorn P, et al. LiFi cross-connection node model using whispering gallery mode of light in a microring resonator. *Microsyst Technol* 2018:1–6.
- [13] Ali J, Youplao P, Pornsuwancharoen N, et al. On-chip electro-optic multiplexing circuit using serial microring boxcar filters. *Results Phys* 2018;10:18–21.
- [14] Pornsuwancharoen N, Amiri IS, Suhailin F, et al. Micro-current source generated by a WGM of light within a stacked silicon-graphene-Au waveguide. *IEEE Photonics Technol Lett* 2017;29:1768–71.
- [15] Youplao P, Pornsuwancharoen N, Amiri IS, et al. Microring stereo sensor model using Kerr-Vernier effect for bio-cell sensor and communication. *Nanocommun Networks* 2018;17:30–5.
- [16] Prabhu AM, Tsay A, Han Z, Van V. Extreme Miniaturization of Silicon Add-Drop Microring Filters for VLSI Photonics Applications. *IEEE Photonics J* 2010;2(3):436–44.